

Decay angular correlations and spectroscopy for $^{10}\text{Be}^* \rightarrow ^4\text{He} + ^6\text{He}$

N. Curtis,* D. D. Caussyn, N. R. Fletcher, F. Maréchal,† N. Fay, and D. Robson
Department of Physics, Florida State University, Tallahassee, Florida 32306-4350
 (Received 23 March 2001; published 20 September 2001)

The $\text{Li}(^7\text{Li}, ^{10}\text{Be}^* \rightarrow ^4\text{He} + ^6\text{He})$ reactions have been studied at bombarding energies of 34 and 50.9 MeV. For $^{10}\text{Be}^*$ production near 0° , decay angular correlations are used to determine the previously unknown spin values and more accurate excitation energies of $J=2$ at $E_x=9.56$ MeV and $J=3$ at $E_x=10.15$ MeV. New excited states are proposed at higher excitations. A triaxial rotor model calculation and other collective rotation proposals all require a $J=4$ state in the vicinity of 9 to 11 MeV, which has not been found. Angular correlation methods more general than have been used in the recent past are discussed.

DOI: 10.1103/PhysRevC.64.044604

PACS number(s): 25.70.-z, 23.60.+e, 21.60.-n

I. INTRODUCTION

As we continue to probe the structure of nuclei further from the line of stability, it becomes increasingly important that we understand quite thoroughly the structure of the more stable next neighboring nuclei. This is particularly true in light nuclei where structure characteristics change so rapidly and systematic changes are much more difficult to establish. In this work we look at a variety of attempts to explain the energy level structure of ^{10}Be and report on α -particle decay angular correlations from excited states of ^{10}Be in an attempt to establish J^π values in support of some of these structure models.

The known energy level structure of ^{10}Be was first compiled by Ajzenberg-Selove and Lauritsen [1] over 40 years ago. The most recent compilation [2] shows that very little information has been added in the intervening years. This paucity of new information extends beyond mere excitation energies, spins, and parities of energy levels to the models for the ^{10}Be structure. In the last few years some new experiments have been performed and new structures have been proposed, which serve as a further motivation for the present investigation.

A distinguishing feature of many collective structure possibilities for ^{10}Be is the location of the first 4^+ state. In a recent extensive study and distorted-wave Born approximation (DWBA) analysis of the $^7\text{Li}(\alpha, p)$ reactions [3], a tentative assignment of 4^+ is given to the excited state at 11.76 MeV, and a rotational band structure is proposed built on the 0^+ ground state. In a second recent work, similar to the present study only at much lower bombarding energy [4], the α -particle decay of excited ^{10}Be is observed. In both of these studies the previous 9.4 MeV state [2] is reported at 9.6 MeV and a new state is observed at 10.2 MeV. This new state is speculated by Soić *et al.* [4] to be the 4^+ member of a rotational band built on the excited 0^+ state at 6.18 MeV. Another collective structure picture for ^{10}Be is obtained by a

comparison with the 3α cluster states of ^{12}C [5] and speculating that a similar structure might be obtained in an α - $2n$ - α cluster structure in ^{10}Be . If we scale the first 2^+ excited state energies in ^{10}Be and ^{12}C , the 0^+ , 7.654 MeV, and 3^- , 9.641 MeV, cluster states in ^{12}C correspond very closely in energy with the 0^+ , 6.179 MeV, and 3^- , 7.371 MeV, states in ^{10}Be . Extrapolation would then predict a 4^+ state in ^{10}Be near 10.7 MeV corresponding to the 4^+ cluster state in ^{12}C at 14.08 MeV. A similar three-cluster orthogonality condition model for ^{10}Be that includes triaxial and quadrupole deformations was carried out some time ago [6], and it predicts the first 4^+ state at approximately 11 MeV in excitation. The model gets the separations of the 0^+ ground state and the first two 2^+ states approximately correct and predicts a 3^+ state at about 9 MeV excitation, but overpredicts the energy of the excited 0^+ , 6.179 MeV, state by 3 MeV.

II. TRIAXIAL MODEL FOR ^{10}Be

Collective excitations based on rotations of a triaxially shaped ground state might be anticipated because of the predicted γ deformation of mass 10 nuclei in a deformed shape-consistent oscillator model [7]. It is possible that triaxiality for ^{10}Be has not been pursued because of the well known expression [8] for the ratio of the excitations of the first two 2^+ states for triaxial collective rotations. In terms of the deformation parameter, γ , the expression is given by

$$\frac{E_{2,2}}{E_{2,1}} = \frac{3 + \sqrt{9 - 8 \sin^2 3\gamma}}{3 - \sqrt{9 - 8 \sin^2 3\gamma}}, \quad (1)$$

showing that the minimum excitation of the second collective 2^+ state is twice that of the first. In ^{10}Be we have 2^+ excitations at 3.368, 5.958, and 7.542 MeV [2]. The predicted [7] value of γ distortion is 34.8° , implying an excitation of the second 2^+ state at 8.00 MeV. If we assume that the 7.542 MeV state actually corresponds to the second 2^+ triaxial collective state, the value of γ from Eq. (1) is 33.8° , which is very close to the predicted value. Pursuing this hypothesis, we have performed a rigid triaxial rotor calculation based on the formalism of Allen and Cross [9]. The resulting

*Present address: School of Physics and Astronomy, University of Birmingham, Edgbaston, Birmingham B15 2TT, United Kingdom.

†Present address: IReS, BP 28, F-67037 Strasbourg Cedex 02, France.

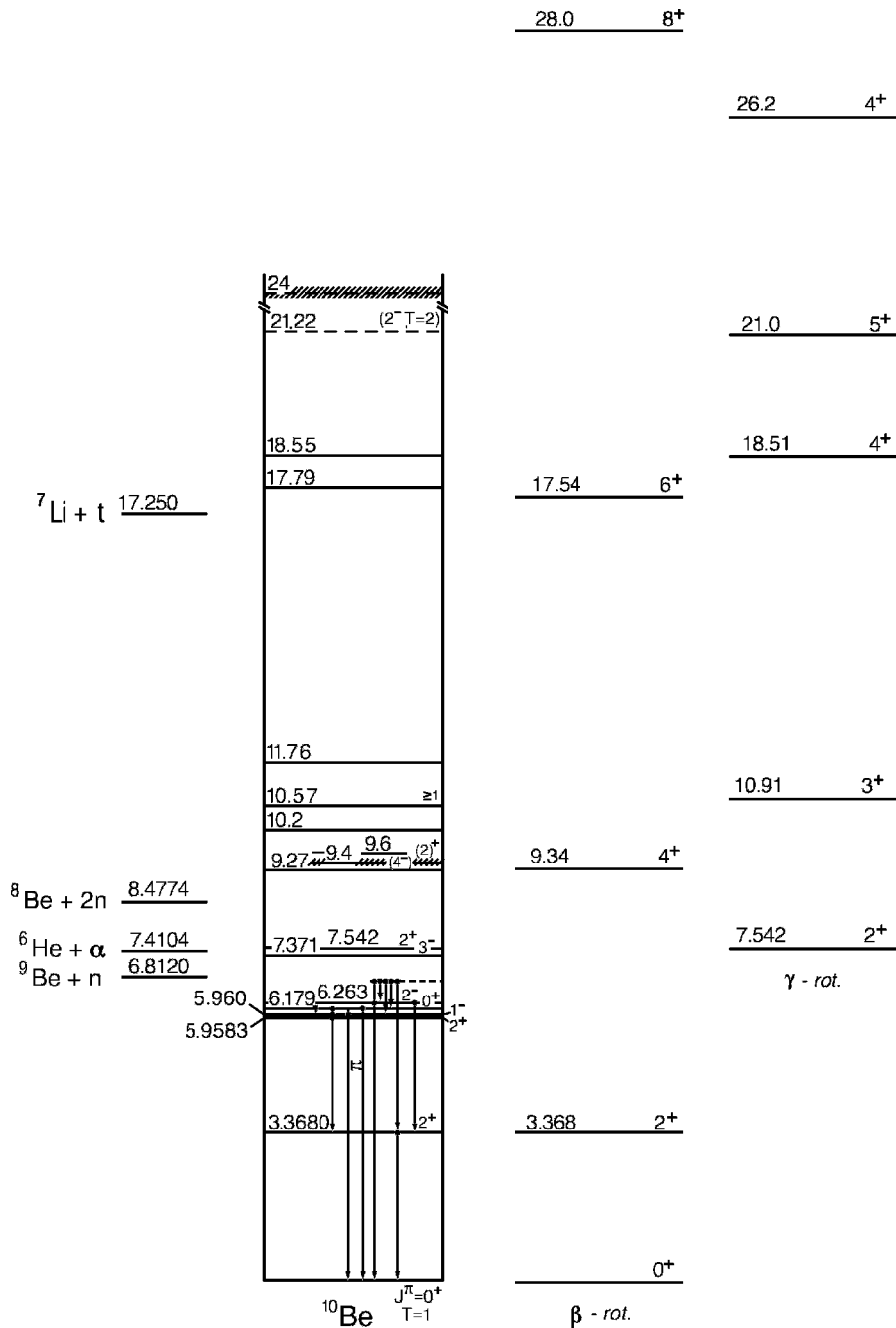


FIG. 1. Excitation energies in ^{10}Be . From left to right: excitation energies for various particle decay processes; energy level diagram for ^{10}Be from Refs. [2–4]; calculated β -rotational band as suppressed by the γ deformation; additional calculated rotational states due exclusively to the γ deformation. The last two columns are based on triaxially deformed rigid rotor calculations.

energy level diagram is compared with the compilation [2] and the more recent results [3,4] in Fig. 1.

There are several intriguing features about this simple model. The large energy gap between excited states from about 11 to 17 MeV is reproduced. The energy positions of the two states just above the triton-decay threshold are nearly independent of the γ distortion parameter, although these energies may be subject to significant change in a calculation in which softness of the nucleus is introduced. The energy position of the first 4^+ state is predicted to be near a region of several known excited states of unknown spin and parity, as was the case of the other proposals [3,4,6]. The triaxial calculation does not describe several known states with ex-

citations of about 6 to 9 MeV, all of which have known spin and parity assignments. It is interesting to note, however, that a single-particle excitation from the closed $1p^{3/2}$ neutron shell to the $1p^{1/2}$ or $1d^{5/2}$ shells would produce negative parity states with $J=1$ through 4 and positive parity states with $J=1$ and 2. These J^π values are all present in the known spectrum except for a missing 1^+ state. Extra states in the known spectrum are the 0^+ state at 6.179 MeV, which has been identified as an intruder state from an early shell model calculation [10], and the other 2^+ state at 7.542 MeV, which we propose as the second triaxial 2^+ state. Lastly, the triaxial rotor model predicts the existence of several high spin states at high excitation energy. This feature alone

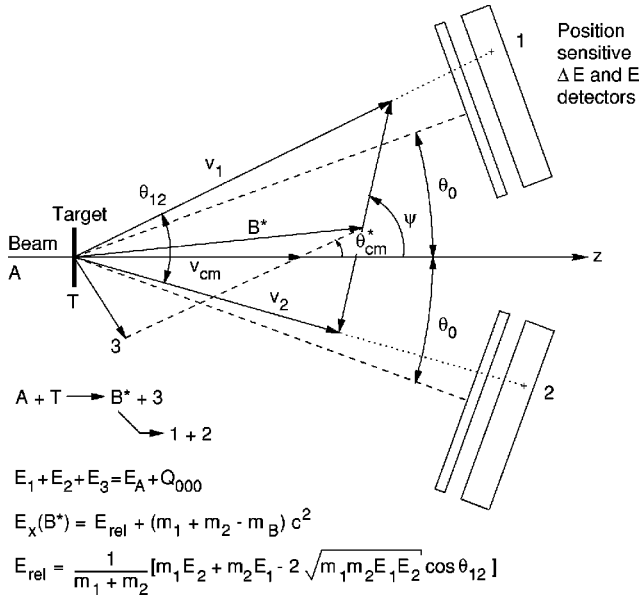


FIG. 2. A velocity addition diagram for three-body final state reactions that proceed by sequential two-body decays, equations for the process, and a schematic of detector placements.

would provide the necessary impetus for further experimental study, although these high spin states may not have a width narrow enough for observation, as has been the case for high spin states in neighboring ^{12}C [11]. Clearly these ideas require support from much more detailed realistic calculations. Our objective is to propose triaxiality as a possible framework for further calculations, and by performing the following experiment, attempt to clarify experimentally the energy level spectroscopy of ^{10}Be .

III. EXPERIMENTAL METHOD AND PROCEDURE

The method of resonant particle decay spectroscopy (RPDS) is well known, and its details are well documented in our previous work [11–13] and references therein. The detector geometry, an explanatory velocity addition diagram, and the equations essential to the method are represented in Fig. 2. The E - ΔE counter telescopes, position sensitive in the horizontal reaction plane, are used to determine the kinetic energy, angular position, and nuclear mass and charge of particles 1 and 2, which are detected in coincidence. From this information and conservation of linear momentum, the energy of the third particle in a three-body final state reaction can be calculated. The sums of the three-particle energies minus the beam energy, for each event, are used to form a Q spectrum to be compared with a calculated Q value for all three particles in their ground states, thus identifying the reaction of interest. A state in the intermediate nucleus, B^* , for sequential binary decay reactions, is identified by peaks in the decay energy (E_{rel}) spectrum. Since the vector addition diagram shown in Fig. 2 is completely known for each event identified as a sequential decay through a state in B^* , the formation and decay angles ($\theta_{c.m.}^*$ and Ψ) are also known for each event and a decay angular correlation can be formed for each excited state of ^{10}Be that can be clearly identified.

The present work is an expansion and update of an earlier preliminary conference proceedings report [14]. The beam in this experiment was ^7Li at energies of 34 and 50.9 MeV. Natural-Li targets with energy thicknesses of 300 to 400 keV were vacuum deposited on thin formvar backings. The detector thicknesses were approximately 67 and 1000 μm for ΔE and E , respectively. Each detector has an active surface area of 10 mm by 50 mm. A rectangular 8 mm by 48 mm collimator is placed in front of the ΔE detectors to limit edge effects and charged-particle-induced radiation damage to the nondepleted region of the silicon wafer. The collimator to target distance is set at 120 mm. The detector centers were nominally set at 18.5° for the 34 MeV experiment, which is designed to investigate the excitation region of about 9 to 14 MeV. These angles are increased to 23° for the 50.9 MeV experiment in order to access a higher excitation region in ^{10}Be .

Detector calibration is critical in these experiments. The α particles from a ^{228}Th radioactive source were used for low-energy calibration. For the higher-energy range calibration the reaction $^{12}\text{C}(^{12}\text{C}, \alpha)$ was used at bombarding energies of 25 and 45 MeV. During the energy calibrations, the position calibration is enacted as well by use of a grid of fixed geometry slits in front of the detectors. Monitor detectors are located above the reaction plane, 16° and 20° from the beam direction, to give measurements of ^7Li and oxygen content in the target. A second monitor, downstream from the target, measures scattering from a secondary gold target to monitor energy loss in the primary target. Each of the two bombarding energy experiments comprised nearly one week of beam on target. Beam current is limited to less than ~ 6 nA such as to preserve position resolution and to produce a true to accidental coincidence ratio of better than 10 to 1.

IV. EXPERIMENTAL RESULTS

A. Energy level spectroscopy of ^{10}Be

The reaction-identifying spectrum for three-body final states following ^7Li bombardment at 34 MeV is shown in Fig. 3. The events near 41 MeV correspond to $^7\text{Li} + ^7\text{Li} \rightarrow ^4\text{He} + ^6\text{He} + ^4\text{He}$, whereas those just below 28 MeV are due to the ^6Li content in the target and correspond to $^6\text{Li} + ^7\text{Li} \rightarrow ^4\text{He} + ^6\text{He} + ^3\text{He}$. The observed energy resolution of about 500 keV represents the net effects of target thickness, straggling, resolution in the four detectors, and position resolution, which determines the accuracy with which the energy of the third final-state particle, the recoil energy (E_{rec}), can be calculated. By selecting the events in Fig. 3 corresponding to the reaction of interest, and similarly for a spectrum at 50.9 MeV bombarding energy, the excitation energy spectra are generated for states in ^{10}Be that are produced in the reaction and then decay into $^4\text{He} + ^6\text{He}$. These spectra are shown in Figs. 4 and 5.

The excitations in ^{10}Be observed in the bombardment of ^7Li are shown in Fig. 4. The excitation energies of 9.56 and 10.15 MeV correspond with those recently identified in Refs. [3,4] as 9.6 and 10.2 MeV. The other two states indicated at 11.8 and 17.8 MeV in excitation have appeared in

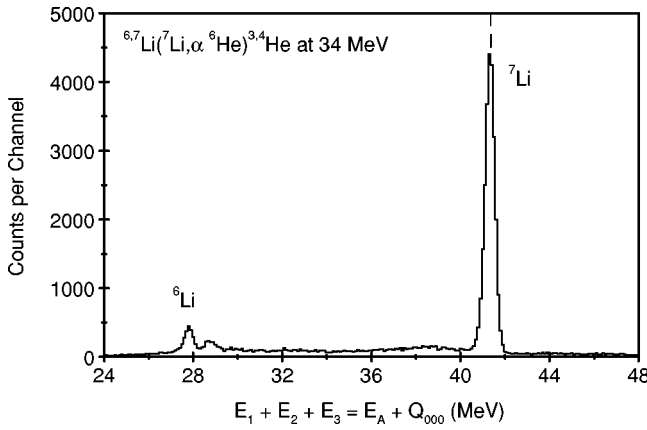


FIG. 3. Experimental Q spectrum for the coincidence detection of ${}^4\text{He}$ and ${}^6\text{He}$. The calculated E_{tot} is the three-body Q value from known masses plus the beam energy. Neglecting the target energy loss effects, the calculated values are 41.37 MeV for a ${}^7\text{Li}$ target and 28.04 MeV for a ${}^6\text{Li}$ target.

the compilations [1,2] for some time. The data from 50.9 MeV bombardment are shown at 200 keV/channel to enhance the observation of any broader structures. Clearly the search for new states in the energy gap between 12 and 17

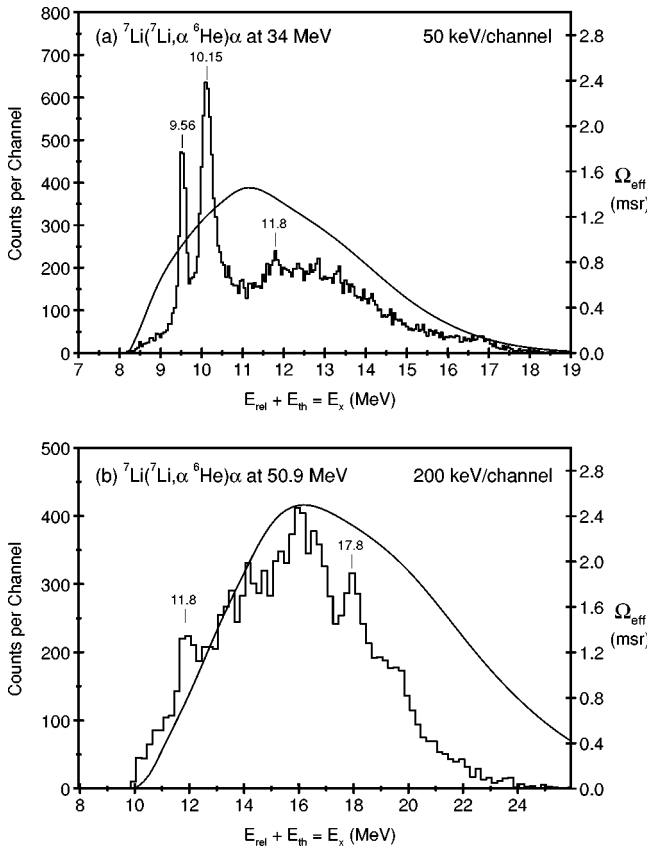


FIG. 4. Excitations in ${}^{10}\text{Be}$ as calculated for each event as $E_{\text{rel}} + E_{\text{th}}$ for the reactions ${}^7\text{Li} + {}^7\text{Li} \rightarrow {}^4\text{He} + {}^6\text{He} + {}^4\text{He}$ at 34.0 and 50.9 MeV. Smooth curves represent the effective solid angles, Ω_{eff} (msr), for the detection of ${}^{10}\text{Be}^*$ decays as calculated by a Monte Carlo simulation. Excited state energies are indicated.

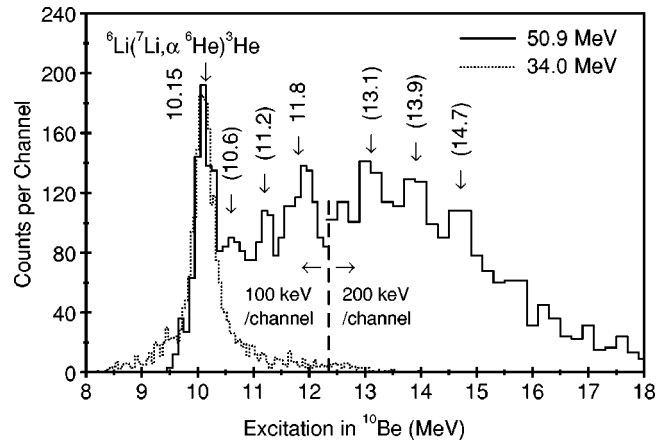


FIG. 5. Excitations in ${}^{10}\text{Be}$ as calculated for each event as $E_{\text{rel}} + E_{\text{th}}$ for the reactions ${}^6\text{Li} + {}^7\text{Li} \rightarrow {}^4\text{He} + {}^6\text{He} + {}^3\text{He}$ at 34.0 and 50.9 MeV. Approximate excited state energies are indicated here and discussed in a later section. The 50.9 MeV data have been multiplied by a factor of 3 at 100 keV/channel, and by a factor of 3/2 at 200 keV/channel. The 34 MeV data are plotted at 50 keV/channel.

MeV and above 20 MeV excitation has not yielded statistically significant results in these spectra. This is in spite of the facts that a positive three-body Q value of over 7 MeV makes these high excitations well within reach and the effective solid angle for detecting the ${}^4\text{He} + {}^6\text{He}$ decay has been ample, ranging from 1.2 to 0.5 msr at these excitations. The continuum, observed in each of the spectra in Fig. 4, is likely due to a combination of the direct production of the three-body final state and sequential two-body decay through highly excited continuum states in ${}^8\text{Be}$.

In the RPDS method the excitation energy resolution in the decaying nucleus improves as the excitation energy decreases approaching threshold. A Monte Carlo code that includes all straggling and resolution effects has been used to determine the decay energy resolution at the location of the 9.56 and 10.15 MeV states, and it yields about 68 and 75 keV, respectively. The experimental data for these states in Fig. 4 clearly show evidence of the natural width of these states. The contributions to the observed widths are the natural widths of Lorentzian line shapes, the Gaussian width of the Monte Carlo energy resolution calculation, and a slight centroid shift of the observed peak with decay angle (Ψ), an effect which is well known [13] but not well understood. After extracting the shift contribution the experimental width values are matched with a convolution of the Gaussian and Lorentzian line shapes to yield natural widths of 141 ± 10 keV for the 9.56 MeV state, and 296 ± 15 keV for the 10.15 MeV state. These widths are about 13 keV less than the previous preliminary values [14], a difference due to this shift contribution.

The excitation spectra for α -particle decaying states in ${}^{10}\text{Be}$ produced from ${}^6\text{Li}$ bombardment are shown in Fig. 5. At a ${}^7\text{Li}$ energy of 50.9 MeV known states are indicated at 10.15, 10.6, and 11.8 MeV, with a possible new state at 11.2 MeV. For higher-energy excitations the data are shown at 200 keV/channel to enhance observation of states of greater width. Here we observe three possible higher energy excita-

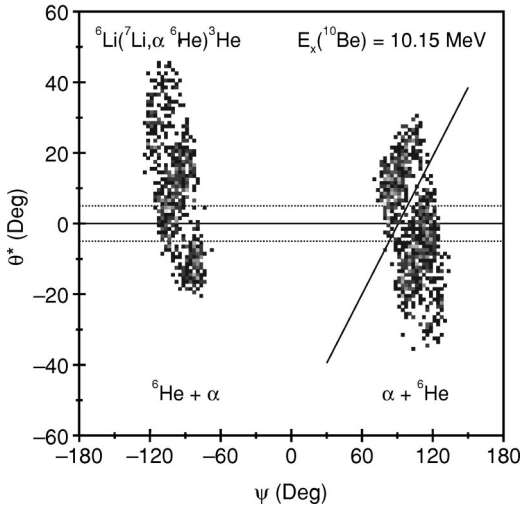


FIG. 6. Event plot of the formation angle θ^* vs the decay angle Ψ for the decay of $^{10}\text{Be}^*(10.15)$ formed by ^6Li bombardment by 34 MeV ^7Li . The two lobes of data represent detection of the α particle to the left or right of the beam, and their lack of symmetry reflects a higher-energy threshold on one of the ΔE detectors. The sloping line, $d\theta^*/d\Psi$, is discussed in the text. The dotted lines indicate the range of data accepted for $\theta^* \approx 0^\circ$ angular correlations.

tions in ^{10}Be . Freer *et al.* [15] have very recently reported similar observations. At 34 MeV bombarding energy, only the 10.15 MeV state appears and its strong isolated yield makes it an excellent candidate for initiating our discussion of decay angular correlations.

B. α -particle decay angular correlations

Each event identified as a specific state in ^{10}Be decaying by α -particle emission is accompanied by the formation angle and decay angle information. Figure 6 shows an event plot for these angles, θ^* and Ψ (see Fig. 2), for the decay of the 10.15 MeV state formed in the ^6Li bombardment by the 34 MeV ^7Li beam (see Fig. 5). Two lobes of data appear corresponding to detecting the ^4He in the detector to the left or right of the beam in coincidence with detecting the ^6He on the opposite side. The lobes have different shapes due to slightly different low-energy cutoffs in the ΔE detectors. A prominently displayed feature of the data is the existence of maxima and minima in the yield, which exhibit a definite slope, $d\theta^*/d\Psi$, as indicated in the figure. This slope effect was first described in a semiclassical explanation by Da Silveira [16] for reactions in which all particles had zero spin. His result gives $d\theta^*/d\Psi \sim J/l_o$, where J is the spin of the decaying state and l_o is the outgoing orbital angular momentum in the formation of the state. The CHARISSA group [17] has used this relationship extensively to assist in determining spin values of decaying states, along with a projection of the data along this slope line onto the $\theta^* = 0^\circ$ axis and comparing the resulting distribution to a $P_J^2(\cos \Psi_0)$.

The slope shown in the data of Fig. 6 ($S=0.65$) indicates $J=3$. In Fig. 7 we show the same data projected onto the $\theta^* = 0^\circ$ axis and compare it with the square of a Legendre polynomial, and that also indicates $J=3$. Again the asymme-

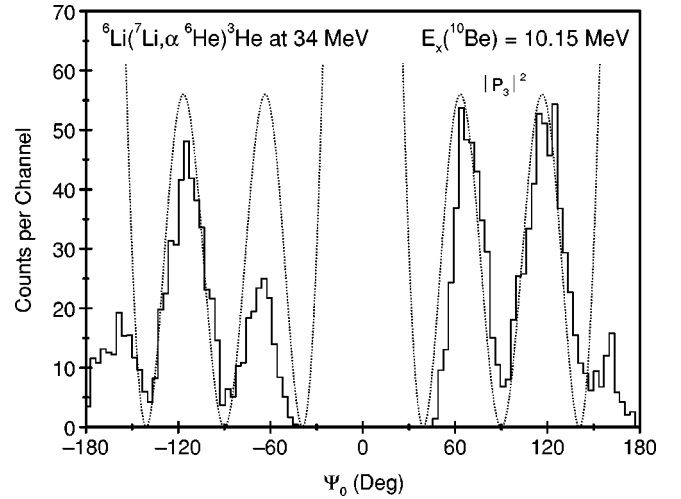


FIG. 7. The events of Fig. 6 projected along the $d\theta^*/d\Psi$ line onto the $\theta^* = 0^\circ$ axis vs $\Psi_0 = \Psi - d\theta^*/d\Psi \Delta\Psi$. The resulting angular correlation is compared with $P_3^2(\cos \Psi_0)$. The data have not been corrected for relative detection efficiency.

try about 0° in Fig. 7 is due to different low-energy cutoffs in the ΔE detectors and these yields have not been corrected for detection efficiency. These slope and Legendre comparisons were formulated for reactions involving all spin-zero particles, yet in our reaction with a variety of possible entrance channel spins, both applications result in $J=3$ for the 10.15 MeV state. This consistent J assignment is undoubtedly due to the fact that the slope property is a limited general property for any state decaying into two spin-zero particles irrespective of the reaction mechanism by which it is formed [18] when using unpolarized beams and targets and in the absence of strong external fields. It depends on the relationship between the modified spherical harmonics of Brink and Satchler [19],

$$C_{Jm}(\theta, 0) = C_{lm} \left(\sqrt{\frac{J(J+1)}{l(l+1)}} \theta, 0 \right), \quad (2)$$

which holds for $|m| < 2$ and to order θ^2 in a power series expansion.

A theoretical expression for fitting the projected correlation (Fig. 7) involving non-spin-zero particles is not available, however for θ^* near 0° , the decay angular correlation versus Ψ is given by [18]

$$W_J(\Psi, \theta^* \sim 0^\circ) = A \sum_{m=0}^{\pm M} p_m^J |C_{Jm}(\Psi, 0^\circ)|^2. \quad (3)$$

The magnetic substate population p_m^J is assumed to be aligned and we approximate it by an exponential falloff in m as

$$p_m^J = e^{-m^2/2\sigma^2} / \sum_{m'=0}^{\pm M} e^{-(m')^2/2\sigma^2}, \quad y = e^{-1/2\sigma^2}. \quad (4)$$

In this parametrization $y=0$ yields $W_J(\Psi, 0) = A[P_J(\cos \Psi)]^2$, and $y=1$ yields isotropy. In the notation

of Fig. 2, $m \equiv m_B = m_A + m_T - m_3 + (m_i - m_o)$, where m_i and m_o are the z components of incoming and outgoing orbital angular momenta. These components are zero at $\theta^* = 0^\circ$. This leads to a maximum possible value of 3 for m , for either of the targets, ${}^6\text{Li}$ or ${}^7\text{Li}$. The summation over m in Eq. (3) is then limited to $M \leq J, 3$. Application of these equations to efficiency-corrected data of Fig. 5, for events in the angular range, $-5^\circ \leq \theta^* \leq +5^\circ$, also results in an assignment of $J = 3$, but as can be seen from Fig. 6 the angular range is small, making an assignment based on this ${}^6\text{Li}$ target data supportive but not very convincing.

The experiment, designed originally for the ${}^7\text{Li} + {}^7\text{Li}$ reactions, results in a much broader Ψ range for the two prominent states shown in the upper portion of Fig. 4. To obtain the angular correlation yields suitable for fitting with Eq. (3) we construct excitation energy spectra for events in 10° intervals in Ψ and for the 10° range in θ^* about 0° . For each of these spectra background-subtracted yields are extracted for the two states in ${}^{10}\text{Be}$. Each yield is then corrected for detection efficiency as calculated by the Monte Carlo code. Although it is possible to have interference between these prominent states and the three-body continuum background seen in Fig. 4(a), we note that these data are very well represented by a smooth background plus Gaussian-broadened Lorentzian line shapes without apparent interference. The individual spectra, gated in 10° intervals in Ψ and θ^* , are of such limited statistical accuracy that attempting to determine interference between the small yields and an even smaller continuum is impractical.

For the α -particle decay of the 10.15 MeV state, the corrected relative yields are shown versus Ψ in Fig. 8, along with a two parameter fit using Eq. (3). The parameters are the relative yield, A , and the magnetic substate mixing factor, y . Both lobes of data in θ versus Ψ space (similar to Fig. 6) are used and the total relative yields are plotted versus $|\Psi|$. The near symmetry about 90° indicates very little interference and the minimum yield at 90° indicates odd J for the state. The use of $J=1$ or 5 resulted in very large values of χ^2/D , where D is the number of degrees of freedom. We

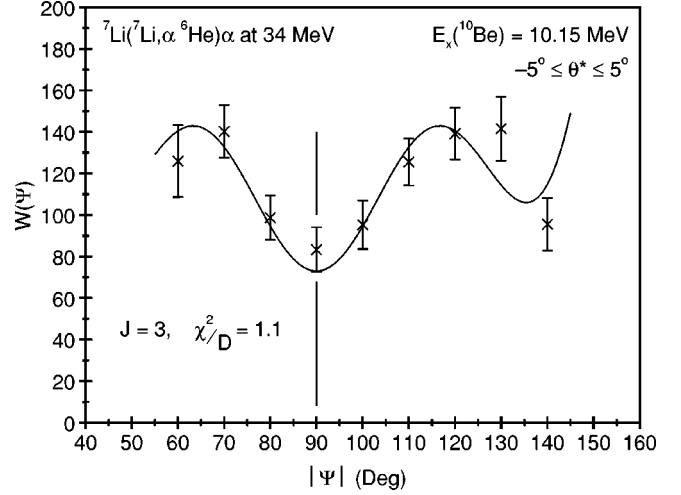


FIG. 8. 0° decay angular correlation for ${}^{10}\text{Be}$ (10.15 MeV) formed by 34 MeV ${}^7\text{Li}$ bombardment of ${}^7\text{Li}$. The relative yields here and in Fig. 9 have been corrected for background and detection efficiency (see text). The solid curve represents the application of Eqs. (3) and (4) with $J=3$ and $y=0.276$.

conclude that $J^\pi = 3^-$ for the 10.15 MeV state, in agreement with all of the analyses of the ${}^6\text{Li}$ target data. The single parameter y determines the relative magnetic substate populations p_m/p_o to be 0.276, 0.006, and $\sim 10^{-5}$, respectively, for $m=1, 2$, and 3 . The dominance of $m=0$ and 1 indicates that a slope line similar to Fig. 6 would also describe these data if it were not for the existence of a large background (Fig. 4) that would fill in the minima.

Data extracted in a similar fashion for the 9.56 MeV state are not symmetric about $\Psi = 90^\circ$, implying positive parity and considerable interference with the 10.15 MeV state. The interference is expected to have a greater effect on the 9.56 MeV state because of the greater strength and width of the interfering state at 10.15 MeV. In a discussion of the two-level interference angular correlation function, we employ the notation of $E_2 = 9.56$ MeV, $E_3 = 10.15$ MeV, J_2 and J_3 for the spins of the states. The correlation function for the 9.56 MeV state is given approximately as [18]

$$\begin{aligned}
 W_{J_2 J_3}(\Psi, \theta^* \sim 0^\circ) &\cong W_{J_2} + F_{23} W_{J_3} + 2 \sqrt{A_2 A_3} F_{23} \sum_{m=0}^{\pm 1} \sqrt{p_m^{J_2} p_m^{J_3}} C_{J_2 m}(\Psi, 0^\circ) C_{J_3 m}(\Psi, 0^\circ) \\
 &\times \left[\cos \delta \left\langle \frac{(E - E_2)(E - E_3) + \frac{1}{4} \Gamma_2 \Gamma_3}{\sqrt{[(E - E_2)^2 + \frac{1}{4} \Gamma_2^2][(E - E_3)^2 + \frac{1}{4} \Gamma_3^2]}} \right\rangle_{\Delta E_2} \right. \\
 &\left. + \sin \delta \left\langle \frac{\frac{1}{2} \Gamma_2 (E - E_3) + \frac{1}{2} \Gamma_3 (E - E_2)}{\sqrt{[(E - E_2)^2 + \frac{1}{4} \Gamma_2^2][(E - E_3)^2 + \frac{1}{4} \Gamma_3^2]}} \right\rangle_{\Delta E_2} \right]. \quad (5)
 \end{aligned}$$

TABLE I. Summary of ^{10}Be spectroscopy, $E_x=9$ to 12 MeV, with recent references. For references prior to 1988, see Ref. [2] and text.

| E_x (MeV) | J^π | $\Gamma_{\text{c.m.}}$ (keV) | Decay | References |
|--------------------|------------|------------------------------|------------------|--------------------|
| 9.27 | (4^-) | 150 ± 20 | n | [2-4] |
| 9.4 | $(2)^+$ | 291 ± 20 | n | [2] |
| 9.64 ± 0.1 | | | | [3] |
| 10.2 | | | | [3] |
| 9.6 ± 0.1 | | | α (n) | [4] |
| 10.2 ± 0.1 | | | α | [4] |
| 9.56 ± 0.02 | 2^+ | 141 ± 10 | α | ^a |
| 10.15 ± 0.02 | 3^- | 296 ± 15 | α | ^a |
| 10.57 | | | n (α) | [2-4] ^a |
| (11.23 ± 0.05) | Nat. π | 200 ± 80^b | (α) | ^a |
| 11.8 | Nat. π | 121 ± 10 | α | [2,3] ^a |

^aPresent work.

^bObserved width, not corrected for system resolution.

The functions W_J are the single level correlation functions of Eq. (3), and the term F_{23} is an integral determining the relative amount of the J_3 correlation that lies within the energy integration window, ΔE_2 , for the J_2 correlation. The remainder of Eq. (5) is the interference term in which δ represents a relative phase between the resonances, averaged over energy and entrance channel spin. Since the $|m|=0,1$ terms dominate the single-level descriptions of the correlation data, the two-level interference correlation functions are appropriately limited to $|m|=0,1$ terms. The other integral terms, $\langle \rangle_{\Delta E_2}$, are also integrated over the energy window ΔE_2 and they involve the natural widths, listed in Table I.

The angular correlation function of Eq. (5) and a similar one with subscripts 2 and 3 interchanged for the 10.15 MeV state are used to describe both sets of data simultaneously in a five-parameter minimization of χ^2/D . The parameters are the two relative amplitudes, A , two substate mixing parameters, y , and the relative average phase. The descriptions of the data are shown in Fig. 9 for spin values of $J_2=2$ and $J_3=3$. Spin values other than $J_2=2$ resulted in much larger values of χ^2/D with a nearly isotropic description of the 9.56 MeV correlation. The relative substate contributions, p_1/p_0 , given by the best fit values of $y_2=0.183$ and $y_3=0.257$ for the 9.56 and 10.15 MeV resonances, respectively, give further justification for limiting the summations to $|m|=0,1$ when using the parametrization of Eq. (4), since the relative substate populations are given by $p_m/p_0=y^{m^2}$.

V. SUMMARY AND DISCUSSION

The spectroscopic information deduced from this experiment at lower excitations of ^{10}Be is compared with recent previous work [3,4] and the compilation [2] in Table I. The J^π values of the 9.56 and 10.15 MeV excited states of ^{10}Be have been unambiguously determined to be 2^+ and 3^- , respectively, and their natural widths have also been measured. The excitation energies quoted are a combination of our results from measurements of the two-body reaction,

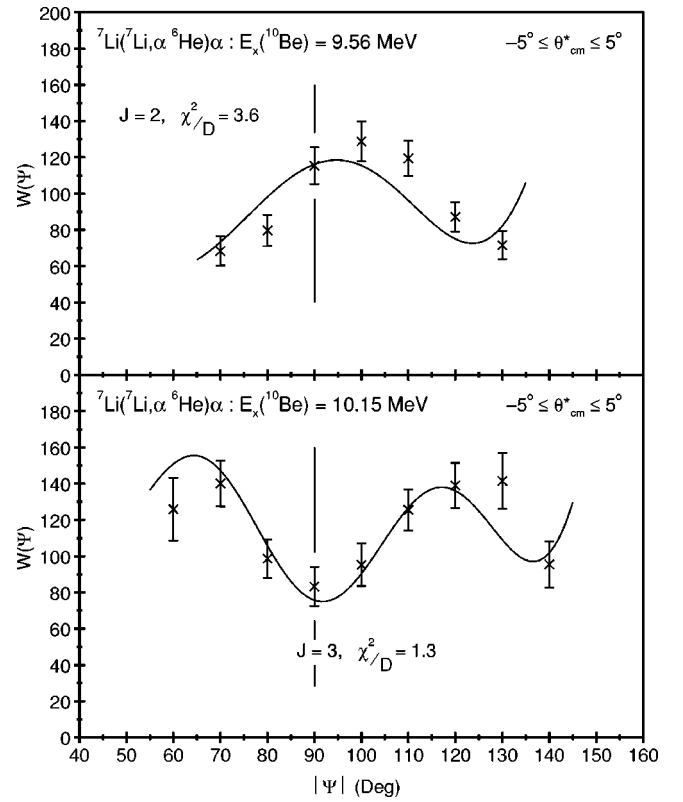


FIG. 9. 0° angular correlations for the decay of the 9.56 and 10.15 MeV states of ^{10}Be formed in 34 MeV ^7Li bombardment of ^7Li . The solid curves are the result of simultaneous application of Eqs. (5) and (4) to both sets of data giving a total value of $\chi^2/D = 2.2$ with $J_2=2$, $J_3=3$, $y_2=0.183$, and $y_3=0.257$.

$^7\text{Li}(^7\text{Li}, \alpha)^{10}\text{Be}$, and the α -particle decay of ^{10}Be excited states. It is clear that these are the same excited states reported in Refs. [3,4]. It is interesting to note that the 9.56 MeV state is not observed from the ^6Li target. This is likely due to the large angular momentum mismatch in that reaction. Our 3^- assignment for the 10.15 MeV state makes invalid the earlier speculation that it could be a 4^+ rotational band member [4]. It does agree well with recent predictions [20,21] of a 3^- state near this excitation. Our tenuous observation of the 10.57 MeV state does not appear convincingly in the α -particle decay of Figs. 4 and 5 or in Ref. [4], whereas it does have a strong neutron decay [4]. Observation of the α -particle decay of the 11.8 MeV state and of a possible new state at 11.2 MeV indicates natural parity.

The excitation energy region above 11.5 MeV is considered in Table II, where we compare the recent result of Freer *et al.* [15] and the present work. The values from this experiment are the result of fitting the data of Fig. 5 at 200 keV/channel with a smooth background plus Gaussian line shapes. The absolute error in our excitation energies is expected to be about ± 0.1 MeV. Even though the excitation energy uncertainties quoted by Freer *et al.* are much larger, there is surprisingly good agreement for three of the four energies. It is disturbing, however, that the 13.85 MeV excitation is not observed in their work. Because of this and the small yields in both experiments, these higher excitations

TABLE II. Comparison of ^{10}Be spectroscopy, $E_x > 11.5$ MeV.

| E_x (MeV) ^b | Present work ^a | | Freer <i>et al.</i> [15] |
|--------------------------|----------------------------|--|--------------------------|
| | Γ_{ob} (keV) | | E_x (MeV) |
| 11.93 | 200 ± 80 ^c | | 11.9 |
| 13.05 | 290 ± 130 | | 13.2 |
| 13.85 | 330 ± 150 | | |
| 14.68 | 310 ± 140 | | 14.8 |
| | | | 16.1 |
| | | | 17.2 |

^aObtained from fitting $E=50.9$ MeV data of Fig. 5 at 200 keV/channel.

^bStatistical uncertainty $\cong 60$ keV, absolute uncertainty $\cong 100$ keV.

^cErrors shown are statistical uncertainties only. These values have not been corrected for system resolution and therefore can only be considered as upper limits (see Sec. V, second paragraph).

must still be treated as tentative new excited states in ^{10}Be . The widths listed in Table II have not been corrected for system resolution and the errors are statistical only. If one assumes that the 11.8 and 11.93 MeV excitations in Tables I and II are the same state, then comparing their widths yields a system resolution of 160 ± 65 keV at this excitation. However, this state indicated at 11.8 MeV in Fig. 5 may be a doublet of 11.76 MeV [2] and 11.95 MeV (see Fig. 5, $E=50.9$ MeV at 100 keV/channel).

A definitive observation of a state at 9.4 MeV has not appeared in recent work. In several experiments a broad (≥ 400 keV) unresolved yield has been observed that encompasses the possible excitations of 9.27, 9.4, and 9.56 MeV [4,22,23]. The original evidence for the 9.4 MeV state is the neutron resonance work of Bockelman *et al.* [22], but even their introduction of this state failed to describe the magnitude of the observed cross section [22] although the 9.27 MeV state is clearly identified. A study of the $^9\text{Be}(\alpha, ^3\text{He})^{10}\text{Be}$ reaction [24] with an energy resolution of 80 keV also failed to resolve these states. Other published works resolve the 9.27 MeV state from a neighboring state at higher excitation [3,25,26]. In the work of Anderson *et al.* [25], $^9\text{Be}(d,p)^{10}\text{Be}$ is the source of the width measurements for states at $E_x=9.27$, 9.4, and 11.76 (see Table I). In their Fig. 1, however, the separation above the 9.27 MeV state

must yield $E_x \sim 9.6$ MeV and not 9.4 MeV for the adjoining member of the doublet [25]. In the proton pickup reaction $^{11}\text{B}(d, ^3\text{He})^{10}\text{Be}$ [26], a single peak is reported in this region at $E_x=9.6$ MeV, yet it has been cited [27] as supporting evidence for the 9.4 MeV state rather than being listed in the compilation as a new state. The absence of the 9.4 MeV state in the proton pickup reaction from the $1p$ shell and the fact that only $J^\pi=0^+$ and 2^+ are observed [26] indicate that if a state exists at 9.4 MeV, it probably has $J \geq 3$. It appears that a neutron capture reaction followed by neutron decay, such as $^9\text{Be}(^7\text{Li}, ^6\text{Li})^{10}\text{Be}^* \rightarrow n + ^9\text{Be}$, with energy resolution equal to or better than the current work will be required to resolve questions remaining about an excited state of ^{10}Be at 9.4 MeV.

The measurements presented in this work do not provide further support for a rigid triaxial rotor description of the excited states of ^{10}Be . The recent molecular orbital model calculation [21] is particularly interesting, since it reproduces many of the features of a triaxial calculation. We can identify their $K^\pi=0^+$ and 2^+ bands with the β and γ rotations of Fig. 1. Due to the increased number of degrees of freedom, their model predicts new bands of excited states. The 9.56 MeV, 2^+ state is probably a member of the $K^\pi=1^+$ band [28] and the 10.15 MeV, 3^- state would belong to the $K^\pi=1^-, 2^-$ band. Higher excitations [21] may correspond with some of the new higher-energy states reported in Table II. Determination of J^π for the states at $E_x=(9.4)$ 10.57, (11.2) 11.8, 17.8, 18.5 MeV and a number of possible new states above 12 MeV will provide further insight into the applicability of this more general model calculation.

ACKNOWLEDGMENTS

This work was supported in part by the National Science Foundation under Grant No. PHY-9523974 and by the Department of Energy under Grant No. DE-FG02-86ER. We also acknowledge the support of Noah Fay, Eastern Michigan University, under the NSF-REU Program, Grant No. PHY-9731605. We would like to thank Daniel Shorb, Powell Barber, and the entire graduate student and technical staff for their help during preparation and the data acquisition phase of the experiment. We also thank Dr. C. Chandler for assistance with the manuscript.

- [1] F. Ajzenberg-Selove and T. Lauritsen, Nucl. Phys. **11**, 1 (1959).
 [2] F. Ajzenberg-Selove, Nucl. Phys. **A490**, 1 (1988).
 [3] S. Hamada, M. Yasue, S. Kubono, M. H. Tanaka, and R. J. Peterson, Phys. Rev. C **49**, 3192 (1994).
 [4] N. Soić, S. Blagus, M. Bogovac, S. Fazinić, M. Lattuada, M. Milin, D. Miljanić, D. Rendić, C. Spitaleri, T. Tadić, and M. Zadro, Europhys. Lett. **34**, 7 (1996).
 [5] D. Robson, Nucl. Phys. **A308**, 301 (1978).
 [6] H. Nishioka, J. Phys. G **10**, 1713 (1984).
 [7] M. Harvey and F. C. Khanna, in *Nuclear Spectroscopy and*

Reactions, Part D, Models of Light Nuclei, edited by J. Cerny (Academic, New York, 1975), p. 69.

- [8] A. S. Davydov and G. F. Filippov, Nucl. Phys. **8**, 237 (1958); Alex Sitenko and Victor Tartakovskii, in *Theory of Nucleus—Nuclear Structure and Nuclear Interactions*, Fundamental Theories of Physics Series, edited by Alwyn Van der Merwe (Kluwer Academic, Dordrecht, Netherlands, 1997), pp. 510–516.
 [9] H. C. Allen, Jr. and P. C. Cross, *Molecular Vib-Rotors* (Wiley, New York, 1963), pp. 16–32, 235.
 [10] A. G. M. van Hees and P. W. M. Glaudemans, Z. Phys. A **315**,

- 223 (1984).
- [11] D. D. Caussyn, G. L. Gentry, J. A. Liendo, N. R. Fletcher, and J. F. Mateja, *Phys. Rev. C* **43**, 205 (1991).
- [12] J. A. Liendo, N. R. Fletcher, E. E. Towers, and D. D. Caussyn, *Phys. Rev. C* **51**, 701 (1995).
- [13] N. R. Fletcher, M. B. Hopson C. Lee, M. A. Tiede, Z. Yang, and J. Liendo, *Nucl. Instrum. Methods Phys. Res. A* **372**, 439 (1996).
- [14] N. Curtis, D. D. Caussyn, N. R. Fletcher, N. Fay, J. A. Liendo, F. Marechal, D. Robson, and D. Shorb, in *Proceedings of the Conference on Nuclear Structure 2000*, edited by T. Glasmacher, P. Mantica, and M. Thoennessen (Elsevier, Amsterdam, 2001); *Nucl. Phys.* **A682**, 339c (2001).
- [15] M. Freer *et al.*, *Phys. Rev. C* **63**, 034301 (2001).
- [16] E. F. Da Silveira, *Proceedings of the Fourteenth Winter Meeting on Nuclear Physics, Bormio, 1976* (unpublished).
- [17] B. R. Fulton, S. J. Bennett, M. Freer, J. T. Murgatroyd, G. J. Gyapong, N. S. Jarvis, C. D. Jones, D. L. Watson, J. D. Brown, W. D. M. Rae, A. E. Smith, and J. S. Lilley, *Phys. Lett. B* **267**, 325 (1991); M. Freer, N. M. Clark, B. R. Fulton, J. T. Murgatroyd, A. St. J. Murphy, S. P. G. Chappell, R. L. Cowin, G. Dillon, D. L. Watson, W. N. Catford, N. Curtis, M. Shawcross, and V. F. E. Pucknell, *Phys. Rev. C* **57**, 1277 (1998).
- [18] D. Robson (unpublished).
- [19] D. M. Brink and G. R. Satchler, *Angular Momentum*, 2nd ed. (Clarendon, Oxford, 1968).
- [20] K. Fujimura, D. Baye, P. Descouvemont, Y. Suzuki, and K. Varga, *Phys. Rev. C* **59**, 817 (1999).
- [21] N. Itagaki and S. Okabe, *Phys. Rev. C* **61**, 044306 (2000).
- [22] C. K. Bockelman, D. W. Miller, R. K. Adair, and H. H. Barshall, *Phys. Rev.* **81**, 69 (1951).
- [23] D. P. Stahel, R. Jahn, G. J. Wozniak, and Joseph Cerny, *Phys. Rev. C* **20**, 1680 (1979); R. B. Weisenmiller, N. A. Jelley, K. H. Wilcox, G. J. Wozniak, and Joseph Cerny, *ibid.* **13**, 1330 (1976).
- [24] M. N. Harakeh, J. Van Porta, A. Saha, and R. H. Siemssen, *Nucl. Phys.* **A344**, 15 (1980).
- [25] R. E. Anderson, J. J. Kraushaar, M. E. Rickey, and W. R. Zimmerman, *Nucl. Phys.* **A236**, 77 (1974).
- [26] U. Schwinn, G. Mairle, G. J. Wagner, and Ch. Ramer, *Z. Phys. A* **275**, 241 (1975).
- [27] F. Ajzenberg-Selove, *Nucl. Phys.* **A320**, 1 (1979).
- [28] N. Itagaki (private communication).